

Supporting Information

for

One-Electron Oxidation of Ferrocenes by Short-Lived *N*-oxyl Radicals. Structural Effects on the Intrinsic Electron Transfer Reactivities of *N*-oxyl Radicals

Enrico Baciocchi, Massimo Bietti, Claudio D'Alfonso, Osvaldo Lanzalunga, Andrea Lapi and
Michela Salamone

Figure S1: Cyclic voltammogram of <i>N</i>-oxyl radicals 1-4 in MeCN	S2
Figure S2: Time-resolved absorption spectra of the dicumyl peroxide/NHQO system	S3
Figures S3-S6: Dependence of k_{obs} for the decay of CumO[•] on the concentration of 1H-4H	S4
Figure S7: Time-resolved absorption spectra of the dicumyl peroxide/NHBO/ethylferrocene carboxylate system	S6
Figure S8. Plots of k_{obs} against [FcX] for the reactions of the MINO radical	S7
Figure S9. Plots of k_{obs} against [FcX] for the reactions of the QONO radical	S7
Figure S10. Plots of k_{obs} against [FcX] for the reactions of the BONO radical	S8
Determination of the reorganization energy	S9
Figure S11. Marcus Plot for the reactions of substituted ferrocenes with MINO	S11
Figure S12. Marcus Plot for the reactions of substituted ferrocenes with BQNO	S11
Figure S13. Marcus Plot for the reactions of substituted ferrocenes with BONO	S12
References for Supporting Information	S13

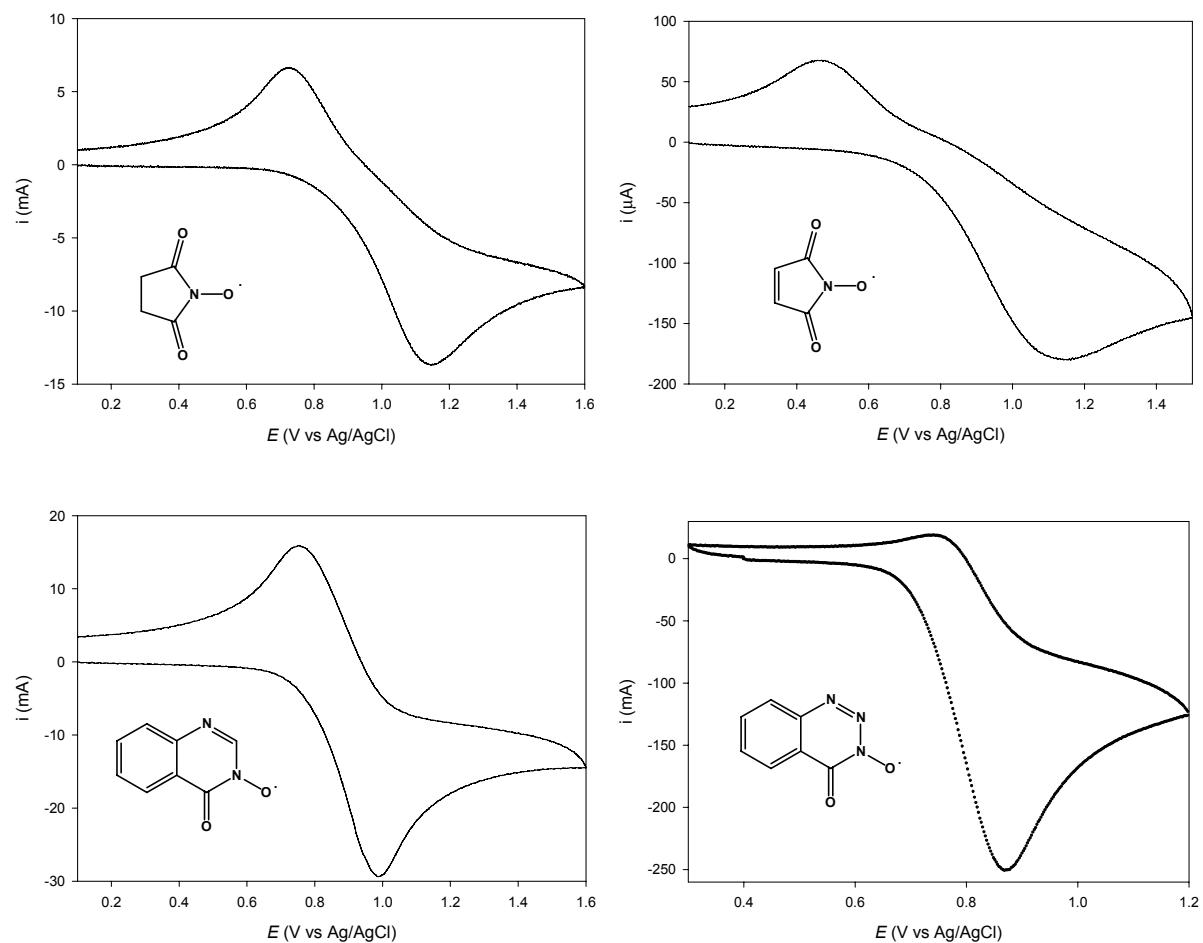


Figure S1. Cyclic voltammogram of 2 mM solutions of *N*-hydroxyderivatives **1H-4H** (2 mM) in MeCN at 25 °C in the presence of collidine (4 mM), containing Bu₄NBF₄ (0.1 M) as the supporting electrolyte. Voltage sweep rate 500 mV/s⁻¹

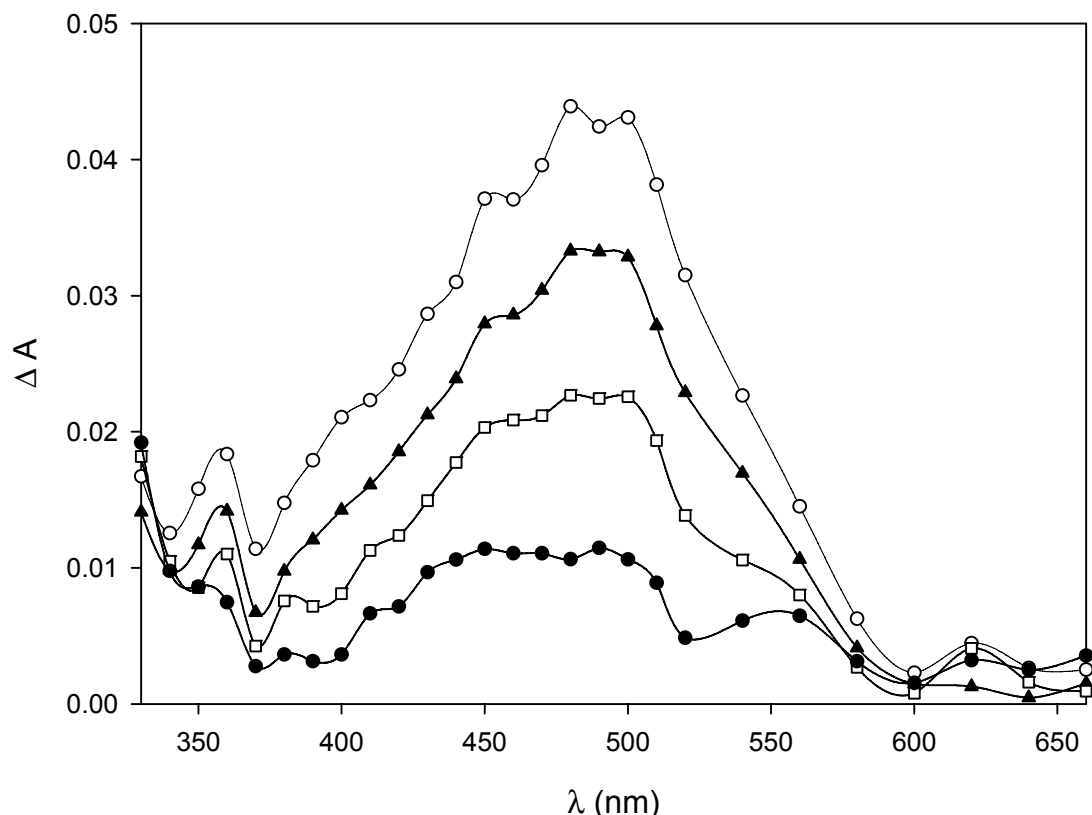


Figure S2. Transient absorption spectra measured 96 ns (empty circles), 416 ns (filled triangles), 1.0 μ s (empty squares) and 3.0 μ s (filled circles) after 355 nm laser excitation of a solution of dicumyl peroxide (0.9 M) and NHQO (2.5 mM) in CH₃CN at 25 °C under N₂

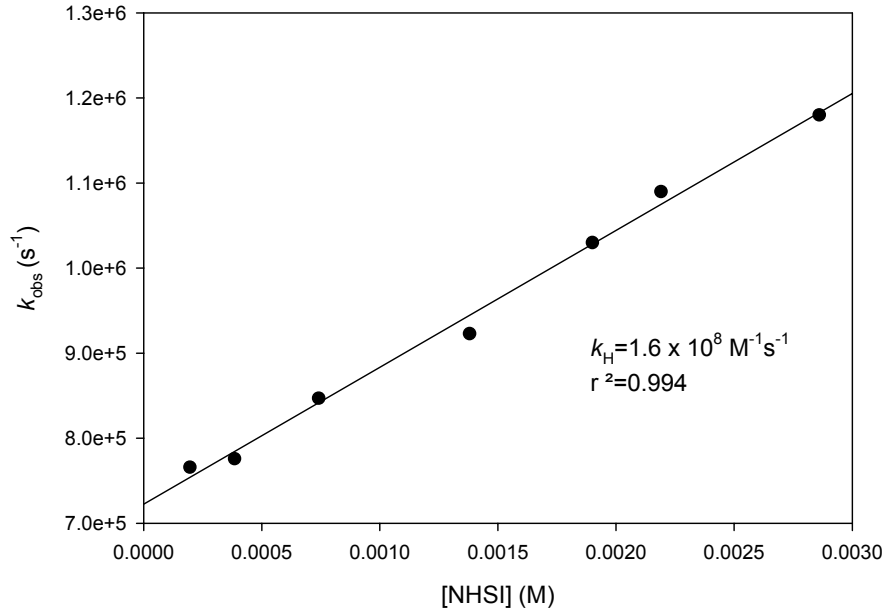


Figure S3. Dependence of k_{obs} on the concentrations of NHSI for the hydrogen atom abstraction from NHSI by the cumyloxy radical in CH_3CN at 25°C .

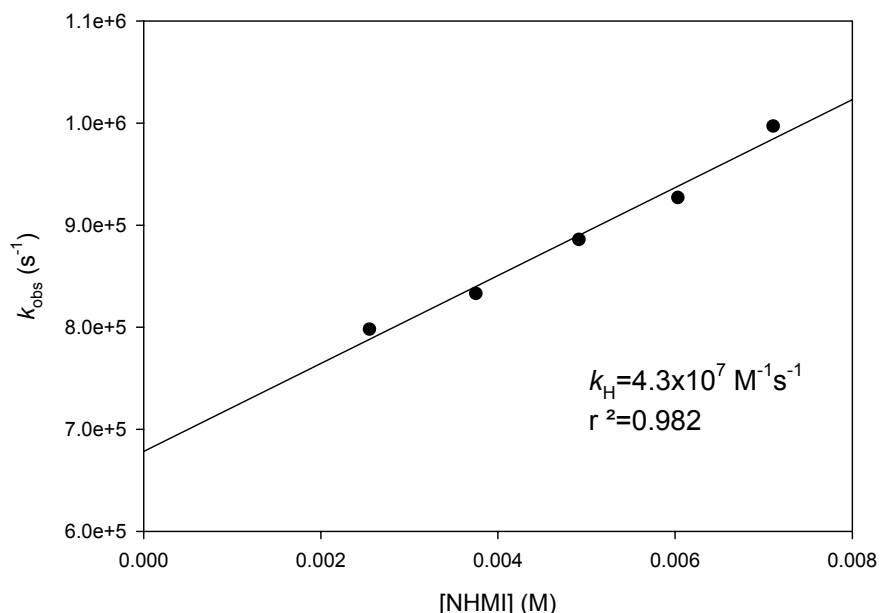


Figure S4. Dependence of k_{obs} on the concentrations of NHMI for the hydrogen atom abstraction from NHMI by the cumyloxy radical in CH_3CN at 25°C .

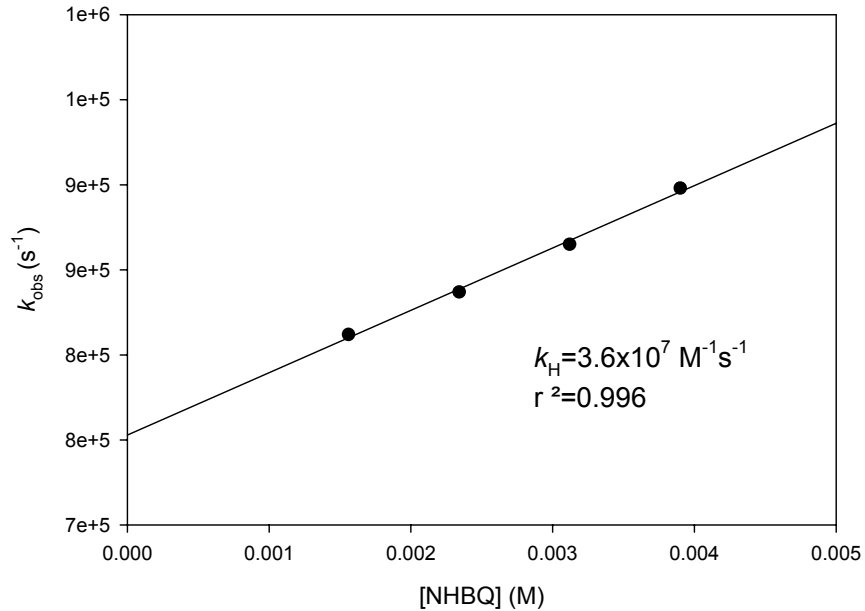


Figure S5. Dependence of k_{obs} on the concentrations of NHBQ for the hydrogen atom abstraction from NHBQ by the cumyloxy radical in CH_3CN at 25°C .

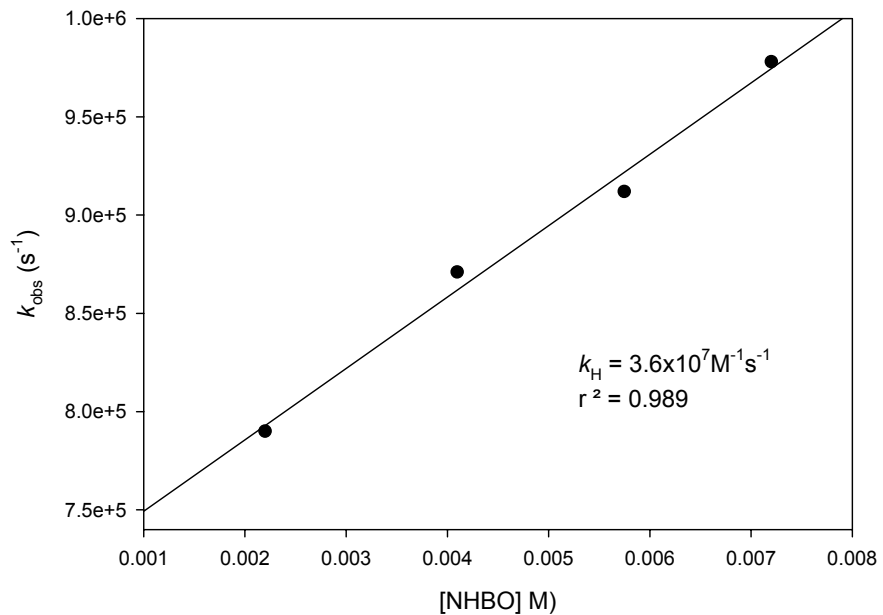


Figure S6. Dependence of k_{obs} on the concentrations of NHBO for the hydrogen atom abstraction from NHBO by the cumyloxy radical in CH_3CN at 25°C .

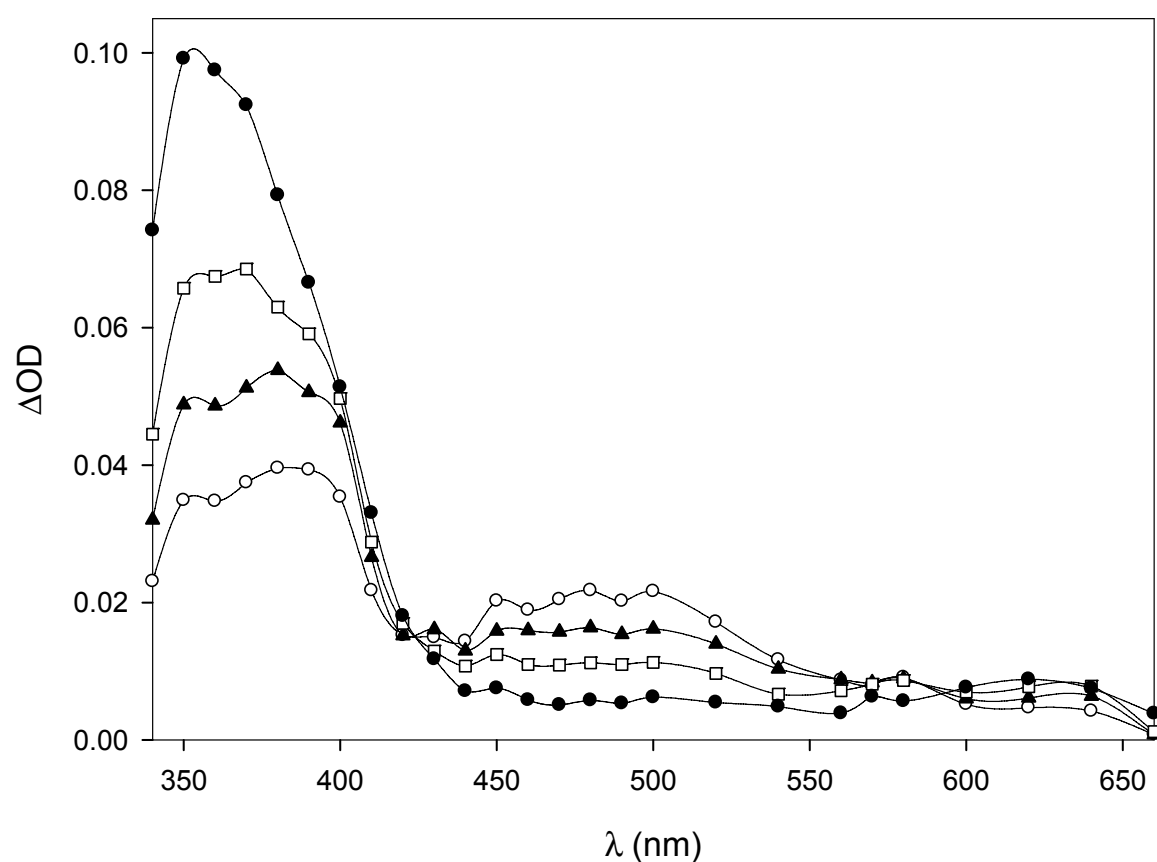


Figure S7. Time-resolved absorption spectra observed after 355 nm LFP of an N_2 -saturated CH_3CN solution ($T = 25^\circ\text{C}$) containing dicumyl peroxide (1 M), NHBO (5.0 mM) and ethylferrocene carboxylate (0.1 mM), at 1.4 μs (empty circles), 4.0 μs (filled triangles), 31 μs (empty squares) and 300 μs (filled circles).

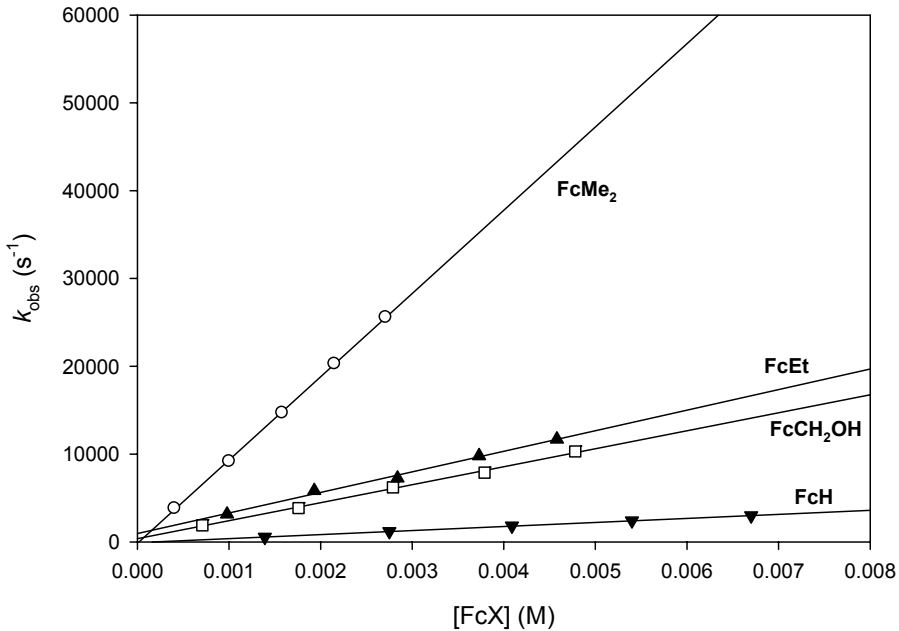


Figure S8. Plots of the observed rate constant (k_{obs}) against $[\text{FcX}]$ for the reactions of the MINO radical measured in argon-saturated MeCN solution at $T = 25$ °C, following the buildup of the ferrocenium ions.

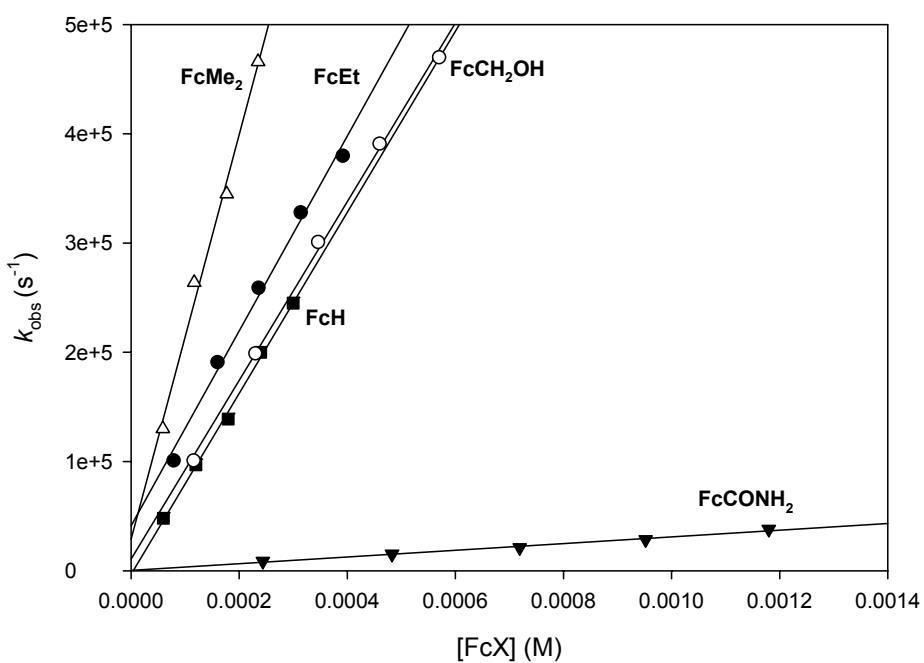


Figure S9. Plots of the observed rate constant (k_{obs}) against $[\text{FcX}]$ for the reactions of the BQNO radical measured in argon-saturated MeCN solution at $T = 25$ °C, following the buildup of the ferrocenium ions.

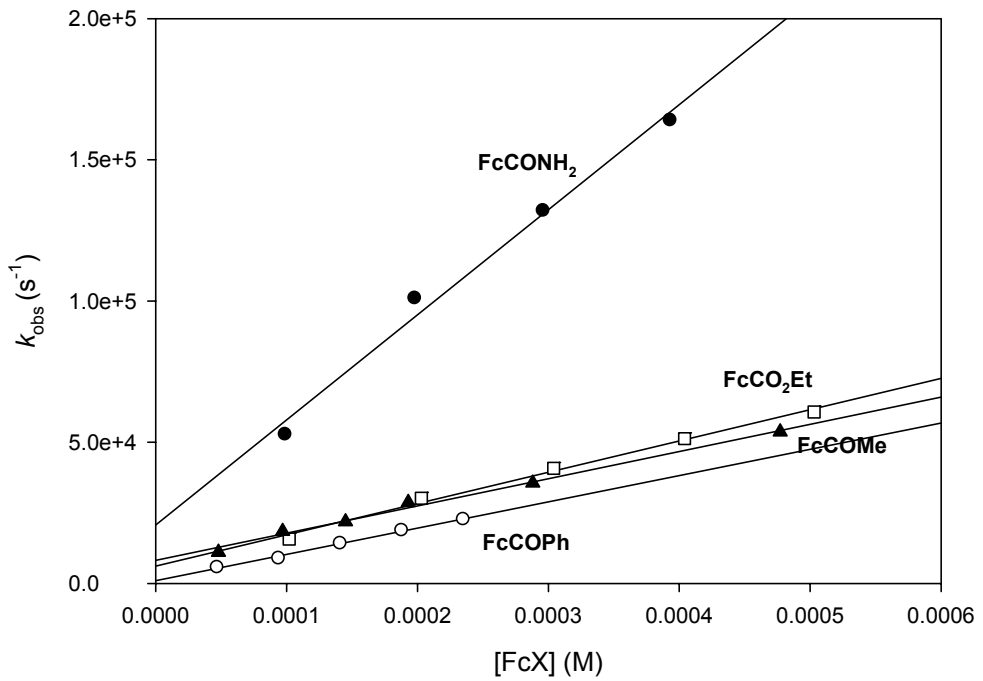


Figure S10. Plots of the observed rate constant (k_{obs}) against $[\text{FcX}]$ for the reactions of the BONO radical measured in argon-saturated MeCN solution at $T = 25 \text{ }^{\circ}\text{C}$, following the decay of the BONO radical.

Determination of the reorganization energies

The second-order rate constants (k_{et}) for the electron transfer process from the substituted ferrocenes FcX to *N*-oxyl radicals **1-4** were treated according to eq 1, which combines the Eyring and Marcus equation.^{S1}

$$k_{et} = Ze^{-\frac{(\lambda + \Delta G^{\circ'})^2}{4\lambda RT}} \quad (1)$$

Z is taken as 6×10^{11} , λ is the reorganization energy representing the energy associated with adjustments in the nuclear geometries and solvent shells of the interacting species which are required to make possible the transfer of the electron from the ferrocene donors to the acceptor *N*-oxyl radicals **1-4** and $\Delta G^{\circ'}$ is the standard free energy for the same step corrected for the electrostatic interaction arising from the charge variation in the reactants upon electron transfer. $\Delta G^{\circ'}$ values are calculated from the ΔG° values reported in Table S1. The ΔG° values have then been corrected for the electrostatic free energy change due to the change in Z_1 and Z_2 upon electron transfer on the basis of eq 2 to give the $\Delta G^{\circ'}$ value to introduce in the eq 1.

$$\Delta G^{\circ'} = \Delta G^{\circ} + (Z_1 - Z_2 - 1)(e^2 f / D r_{12}) \quad (2)$$

In eq 2, e is the electron charge, Z_1 and Z_2 are the charge numbers of the reactants, r_{12} is the distance between *N*-oxyl radicals **1-4** and the ferrocenes in the encounter complex (taken as 7.0 Å for SINO and MINO radicals and 7.4 Å for QONO and BONO radicals),^{S2} D is the dielectric constant of the solvent (35 for CH₃CN), and f is a factor depending upon the ionic strength ($f \equiv 1$ for $\mu \rightarrow 0$). The values of $\Delta G^{\circ'}$ evaluated as described above are listed in Table S1. These values refer to reactions carried out at 25 °C.

Nonlinear least squares curve fitting of the experimental data has been carried out using the reorganization energy λ as adjustable parameter. The best fit of the experimental data with the curve

calculated by eq 1 (Figure 7 and Figures S10-S12) are obtained for λ values of 43.6 kcal mol⁻¹ (**1**), 49.3 kcal mol⁻¹ (**2**), 36.0 kcal mol⁻¹ (**3**) and 28.4 kcal mol⁻¹ (**4**).

Table S1. Standard free energy (ΔG°) and standard free energy corrected for the electrostatic contribution ($\Delta G^\circ'$) for the electron transfer from ferrocenes (FcX) to *N*-oxyl radicals **1-4** at 25 °C in CH₃CN.

FcX	SINO (1)		MINO (2)		QONO (3)		BONO (4)	
	ΔG°	$\Delta G^\circ'$						
FcH	-11.7	-13.1	-8.2	-9.6	-9.9	-11.2		
FcMe₂	-14.4	-15.8	-11.0	-12.4	-12.7	-14.0		
FcEt	-13.3	-14.7	-9.8	-11.2	-11.5	-12.8		
FcCH₂OH	-11.9	-13.3	-8.4	-9.8	-10.1	-11.4		
FcCONH₂	-7.7	-9.1			-6.0	-7.3	-4.4	-5.7
FcCO₂Et	-6.1	-7.5					-2.8	-4.1
FcCOMe							-2.5	-3.8
FcCOPh							-1.9	-3.2

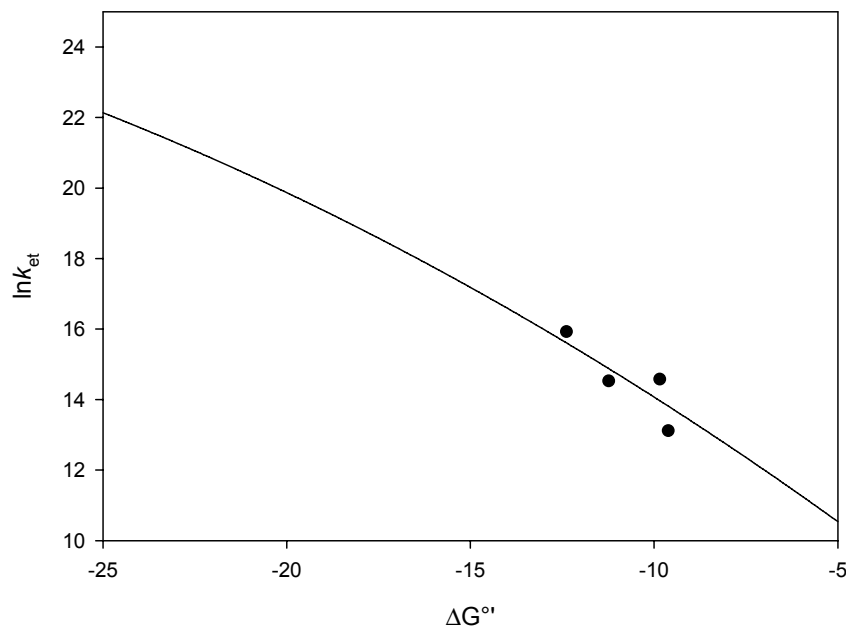


Figure S11. Diagram of $\ln k_{\text{et}}$ vs ΔG° for the reactions of substituted ferrocenes with MINO. The solid circles correspond to the experimental values; the curve is calculated by nonlinear least-squares fit to eq 1.

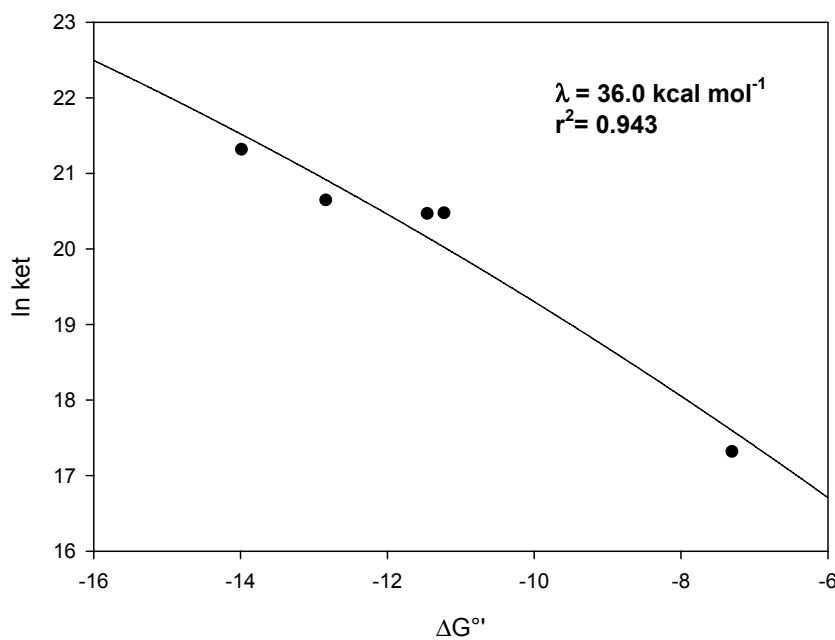


Figure S12. Diagram of $\ln k_{\text{et}}$ vs ΔG° for the reactions of substituted ferrocenes with QONO. The solid circles correspond to the experimental values; the curve is calculated by nonlinear least-squares fit to eq 1.

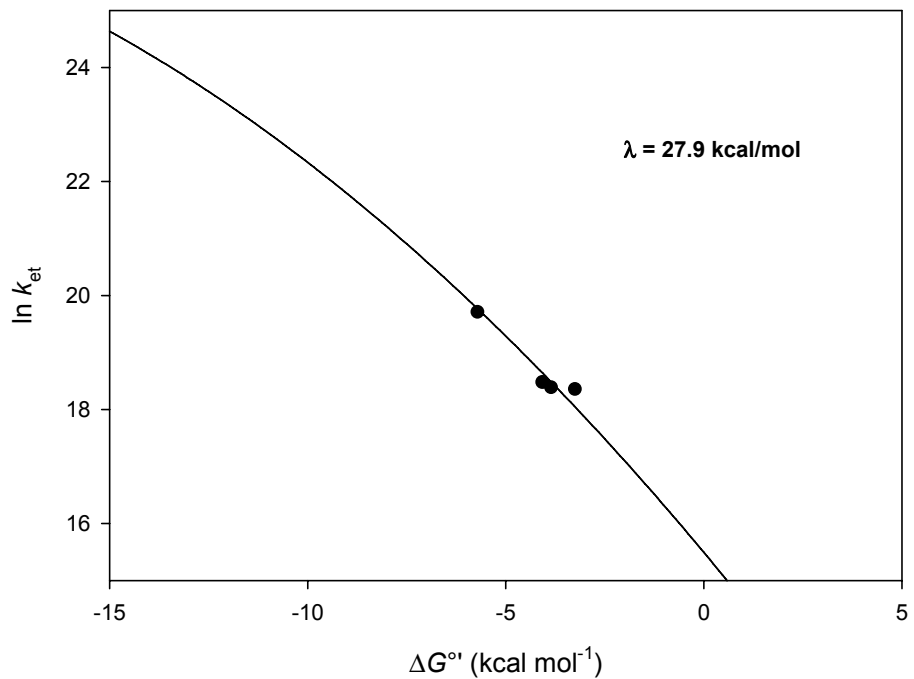


Figure S13. Diagram of $\ln k_{et}$ vs $\Delta G^{\circ\prime}$ for the reactions of substituted ferrocenes with BONO. The solid circles correspond to the experimental values; the curve is calculated by nonlinear least-squares fit to eq 1.

References for Supporting Information

- S1. Eberson, L. *Electron Transfer Reactions in Organic Chemistry*; Springer Verlag: Berlin Heidelberg, 1986; Chapter 3.
- S2. The radius of ferrocene (2.6 Å) is taken from ref. S3. The radii of SINO and MINO (4.4 Å) and QONO and BONO (4.8 Å) were calculated from the volume of the *N*-oxyl radicals given by the Hyperchem program.
- S3. Carlson, B. W.; Miller, L. L.; Neta, P.; Grodkowski, J. *J. Am. Chem. Soc.*, **1984**, *103*, 7233.
- S4. Baciocchi, E.; Bietti, M.; Gerini, M. F.; Lanzalunga O. *J. Org. Chem.* **2005**, *70*, 5144-5149.